9-1-1999

Measurement of the $B_d^0 \bar{B}_d^0$ oscillation frequency using dimuon data in $p\bar{p}$ collisions at √s =1.8TeV

F. Abe
National Laboratory for High Energy Physics (KEK), Tsukuba, Ibaraki 305, Japan

Kenneth A. Bloom
University of Nebraska-Lincoln, kenbloom@unl.edu

Collider Detector at Fermilab Collaboration

PHYSICAL REVIEW D, VOLUME 60, 051101

Measurement of the $B_d^0\overline{B}_d^0$ oscillation frequency using dimuon data in $p\overline{p}$ collisions at $\sqrt{s}=1.8$ TeV

F. Abe,[17] H. Akimoto,[39] A. Akopian,[31] M. G. Albrow,[7] S. R. Amendolia,[27] D. Amidei,[20] J. Antos,[33] S. Aota,[37] G. Apollinari,[31] T. Arisawa,[39] T. Asakawa,[37] W. Ashmanskas,[5] M. Atac,[7] P. Azzi-Bacchetta,[25] N. Bacchetta,[25] S. Bagdasarov,[31] M. W. Bailey,[22] P. de Barbaro,[30] A. Barbaro-Galtieri,[18] V. E. Barnes,[29] B. A. Barnett,[15] M. Barone,[9] G. Bauer,[19] T. Baumann,[11] F. Bedeschi,[27] S. Behrends,[3] S. Belforte,[27] G. Bellettini,[27] J. Bellinger,[40] D. Benjamin,[6] J. Bensinger,[3] A. Beretvas,[7] J. P. Berge,[7] J. Berryhill,[5] S. Bertolucci,[9] S. Bettelli,[27] B. Bevensee,[26] A. Bhatti,[31] K. Biery,[7] C. Bigongiari,[27] M. Binkley,[7] D. Bisello,[25] R. E. Blair,[1] C. Blocker,[3] K. Bloom,[20] S. Blusk,[30] A. Bodek,[30] W. Bokhari,[26] G. Bolla,[29] Y. Bonushkin,[4] D. Bortoletto,[29] J. Boudreau,[28] A. Brandl,[22] L. Breccia,[2] C. Bromberg,[21] N. Bruner,[22] R. Brunetti,[2] E. Buckley-Geer,[7] H. S. Budd,[30] K. Burkett,[11] G. Busetto,[25] A. Byon-Wagner,[7] K. L. Byrum,[1] M. Campbell,[20] A. Caner,[27] W. Carithers,[18] D. Carlsmith,[40] J. Cassada,[30] A. Castro,[25] D. Cauz,[36] A. Cerri,[27] P. S. Chang,[33] P. T. Chang,[33] H. Y. Chao,[33] J. Chapman,[20] M. -T. Cheng,[33] M. Chertok,[34] G. Chiarelli,[27] C. N. Chiou,[33] F. Chlebana,[7] L. Christofek,[13] M. L. Chu,[33] S. Cihangir,[7] A. G. Clark,[10] M. Cobal,[27] E. Cocca,[27] M. Contreras,[5] J. Conway,[32] J. Cooper,[7] M. Cordelli,[9] D. Costanzo,[27] C. Couyoumtzelis,[10] D. Cronin-Hennessy,[6] R. Cropp,[14] R. Culbertson,[5] D. Dagenhart,[38] T. Daniels,[19] F. DeJongh,[7] S. Dell'Agnello,[9] M. Dell'Orso,[27] R. Demina,[7] L. Demortier,[31] M. Deninno,[2] P. F. Derwent,[7] T. Devlin,[32] J. R. Dittmann,[6] G. Dolce,[25] S. Donati,[27] J. Done,[34] T. Dorigo,[25] N. Eddy,[13] K. Einsweiler,[18] J. E. Elias,[7] R. Ely,[18] E. Engels, Jr.,[28] W. Erdmann,[7] D. Errede,[13] S. Errede,[13] Q. Fan,[30] R. G. Feild,[41] Z. Feng,[15] C. Ferretti,[27] I. Fiori,[2] B. Flaugher,[7] G. W. Foster,[7] M. Franklin,[11] J. Freeman,[7] J. Friedman,[19] H. Frisch,[5] Y. Fukui,[17] S. Gadomski,[14] S. Galeotti,[27] M. Gallinaro,[26] O. Ganel,[35] M. Garcia-Sciveres,[18] A. F. Garfinkel,[29] C. Gay,[41] S. Geer,[7] D. W. Gerdes,[20] P. Giannetti,[27] N. Giokaris,[31] P. Giromini,[9] G. Giusti,[27] M. Gold,[22] A. Gordon,[11] A. T. Goshaw,[6] Y. Gotra,[28] K. Goulianos,[31] H. Grassmann,[36] C. Green,[29] L. Groer,[32] C. Grosso-Pilcher,[5] G. Guillian,[20] J. Guimaraes da Costa,[15] R. S. Guo,[33] C. Haber,[18] E. Hafen,[19] S. R. Hahn,[7] R. Hamilton,[11] T. Handa,[12] R. Handler,[40] W. Hao,[35] F. Happacher,[9] K. Hara,[37] A. D. Hardman,[29] R. M. Harris,[7] F. Hartmann,[16] J. Hauser,[4] E. Hayashi,[37] J. Heinrich,[26] A. Heiss,[16] B. Hinrichsen,[14] K. D. Hoffman,[29] C. Holck,[26] R. Hollebeek,[26] L. Holloway,[13] Z. Huang,[20] B. T. Huffman,[28] R. Hughes,[23] J. Huston,[21] J. Huth,[11] H. Ikeda,[37] M. Incagli,[27] J. Incandela,[7] G. Introzzi,[27] J. Iwai,[39] Y. Iwata,[12] E. James,[20] H. Jensen,[7] U. Joshi,[7] E. Kajfasz,[25] H. Kambara,[10] T. Kamon,[34] T. Kaneko,[37] K. Karr,[38] H. Kasha,[41] Y. Kato,[24] T. A. Keaffaber,[29] K. Kelley,[19] M. Kelly,[20] R. D. Kennedy,[7] R. Kephart,[7] D. Kestenbaum,[11] D. Khazins,[6] T. Kikuchi,[37] M. Kirk,[3] B. J. Kim,[27] H. S. Kim,[14] S. H. Kim,[37] Y. K. Kim,[18] L. Kirsch,[3] S. Klimenko,[8] D. Knoblauch,[16] P. Koehn,[23] A. Köngeter,[16] K. Kondo,[37] J. Konigsberg,[8] K. Kordas,[14] A. Korytov,[8] E. Kovacs,[1] W. Kowald,[6] J. Kroll,[26] M. Kruse,[30] S. E. Kuhlmann,[1] E. Kuns,[32] K. Kurino,[12] T. Kuwabara,[37] A. T. Laasanen,[29] S. Lami,[27] S. Lammel,[7] J. I. Lamoureux,[3] M. Lancaster,[18] M. Lanzoni,[27] G. Latino,[27] T. LeCompte,[1] A. M. Lee IV,[6] S. Leone,[27] J. D. Lewis,[7] M. Lindgren,[4] T. M. Liss,[13] J. B. Liu,[30] Y. C. Liu,[33] N. Lockyer,[26] O. Long,[26] M. Loreti,[25] D. Lucchesi,[27] P. Lukens,[7] S. Lusin,[40] J. Lys,[18] K. Maeshima,[7] P. Maksimovic,[11] M. Mangano,[27] M. Mariotti,[25] J. P. Marriner,[7] G. Martignon,[25] A. Martin,[41] J. A. J. Matthews,[22] P. Mazzanti,[2] K. McFarland,[30] P. McIntyre,[34] P. Melese,[31] M. Menguzzato,[25] A. Menzione,[27] E. Meschi,[27] S. Metzler,[26] C. Miao,[20] T. Miao,[7] G. Michail,[11] R. Miller,[21] H. Minato,[37] S. Miscetti,[9] M. Mishina,[17] S. Miyashita,[37] N. Moggi,[27] E. Moore,[22] Y. Morita,[17] A. Mukherjee,[7] T. Muller,[16] A. Munar,[27] P. Murat,[27] S. Murgia,[21] M. Musy,[36] H. Nakada,[37] T. Nakaya,[5] I. Nakano,[12] C. Nelson,[7] D. Neuberger,[16] C. Newman-Holmes,[7] C.-Y. P. Ngan,[19] H. Niu,[3] L. Nodulman,[1] A. Nomerotski,[8] S. H. Oh,[6] T. Ohmoto,[12] T. Ohsugi,[12] R. Oishi,[37] M. Okabe,[37] T. Okusawa,[24] J. Olsen,[40] C. Pagliarone,[27] R. Paoletti,[27] V. Papadimitriou,[35] S. P. Pappas,[41] N. Parashar,[27] A. Parri,[9] D. Partos,[3] J. Patrick,[7] G. Pauletta,[36] M. Paulini,[18] A. Perazzo,[27] L. Pescara,[25] M. D. Peters,[18] T. J. Phillips,[6] G. Piacentino,[27] M. Pillai,[30] K. T. Pitts,[7] R. Plunkett,[7] A. Pompos,[29] L. Pondrom,[40] J. Proudfoot,[1] F. Ptohos,[11] G. Punzi,[27] K. Ragan,[14] D. Reher,[18] A. Ribon,[25] F. Rimondi,[2] L. Ristori,[27] W. J. Robertson,[6] A. Robinson,[14] T. Rodrigo,[27] S. Rolli,[38] L. Rosenson,[19] R. Roser,[7] T. Saab,[14] W. K. Sakumoto,[30] D. Saltzberg,[4] A. Sansoni,[9] L. Santi,[36] H. Sato,[37] P. Schlabach,[7] E. E. Schmidt,[7] M. P. Schmidt,[41] A. Scott,[4] A. Scribano,[27] S. Segler,[7] S. Seidel,[22] Y. Seiya,[37] F. Semeria,[2] T. Shah,[19] M. D. Shapiro,[18] N. M. Shaw,[29] P. F. Shepard,[28] T. Shibayama,[37] M. Shimojima,[37] M. Shochet,[5] J. Siegrist,[18] A. Sill,[35] P. Sinervo,[14] P. Singh,[13] K. Sliwa,[38] C. Smith,[15] F. D. Snider,[7] J. Spalding,[7] T. Speer,[10] P. Sphicas,[19] F. Spinella,[27] M. Spiropulu,[11] L. Spiegel,[7] L. Stanco,[25] J. Steele,[40] A. Stefanini,[27] R. Ströhmer,[7,*] J. Strologas,[13] F. Strumia,[10] D. Stuart,[7] K. Sumorok,[19] J. Suzuki,[37] T. Suzuki,[37] T. Takahashi,[24] T. Takano,[24] R. Takashima,[12] K. Takikawa,[37] M. Tanaka,[37] B. Tannenbaum,[4] F. Tartarelli,[27] W. Taylor,[14] M. Tecchio,[20] P. K. Teng,[33] Y. Teramoto,[24] K. Terashi,[37] S. Tether,[19] D. Theriot,[7] T. L. Thomas,[22] R. Thurman-Keup,[1] M. Timko,[38] P. Tipton,[30] A. Titov,[31] S. Tkaczyk,[7] D. Toback,[5] K. Tollefson,[30] A. Tollestrup,[7] H. Toyoda,[24] W. Trischuk,[14] J. F. de Troconiz,[11] S. Truitt,[20] J. Tseng,[19] N. Turini,[27] T. Uchida,[37] F. Ukegawa,[26] J. Valls,[32] S. C. van den Brink,[15] S. Vejcik III,[7] G. Velev,[27] R. Vidal,[7] R. Vilar,[7,*] I. Vologouev,[18] D. Vucinic,[19] R. G. Wagner,[1] R. L. Wagner,[7] J. Wahl,[5] N. B. Wallace,[27] A. M. Walsh,[32] C. Wang,[6] C. H. Wang,[33] M. J. Wang,[33] A. Warburton,[14] T. Watanabe,[37] T. Watts,[32] R. Webb,[34] C. Wei,[6] H. Wenzel,[16] W. C. Wester III,[7] A. B. Wicklund,[1] E. Wicklund,[7] R. Wilkinson,[26] H. H. Williams,[26] P. Wilson,[7] B. L. Winer,[23] D. Winn,[20] D. Wolinski,[20] J. Wolinski,[21] S. Worm,[22] X. Wu,[10] J. Wyss,[27] A. Yagil,[7] W. Yao,[18] K. Yasuoka,[37] G. P. Yeh,[7] P. Yeh,[33] J. Yoh,[7] C. Yosef,[21] T. Yoshida,[24] I. Yu,[7] A. Zanetti,[36] F. Zetti,[27] and S. Zucchelli[2]

(CDF Collaboration)
[1]*Argonne National Laboratory, Argonne, Illinois 60439*
[2]*Istituto Nazionale di Fisica Nucleare, University of Bologna, I-40127 Bologna, Italy*
[3]*Brandeis University, Waltham, Massachusetts 02254*
[4]*University of California at Los Angeles, Los Angeles, California 90024*
[5]*University of Chicago, Chicago, Illinois 60637*
[6]*Duke University, Durham, North Carolina 27708*
[7]*Fermi National Accelerator Laboratory, Batavia, Illinois 60510*
[8]*University of Florida, Gainesville, Florida 32611*
[9]*Laboratori Nazionali di Frascati, Istituto Nazionale di Fisica Nucleare, I-00044 Frascati, Italy*
[10]*University of Geneva, CH-1211 Geneva 4, Switzerland*
[11]*Harvard University, Cambridge, Massachusetts 02138*
[12]*Hiroshima University, Higashi-Hiroshima 724, Japan*
[13]*University of Illinois, Urbana, Illinois 61801*
[14]*Institute of Particle Physics, McGill University, Montreal, Quebec, Canada H3A 2T8 and University of Toronto, Toronto, Ontario, Canada M5S 1A7*
[15]*The Johns Hopkins University, Baltimore, Maryland 21218*
[16]*Institut für Experimentelle Kernphysik, Universität Karlsruhe, 76128 Karlsruhe, Germany*
[17]*National Laboratory for High Energy Physics (KEK), Tsukuba, Ibaraki 305, Japan*
[18]*Ernest Orlando Lawrence Berkeley National Laboratory, Berkeley, California 94720*
[19]*Massachusetts Institute of Technology, Cambridge, Massachusetts 02139*
[20]*University of Michigan, Ann Arbor, Michigan 48109*
[21]*Michigan State University, East Lansing, Michigan 48824*
[22]*University of New Mexico, Albuquerque, New Mexico 87131*
[23]*The Ohio State University, Columbus, Ohio 43210*
[24]*Osaka City University, Osaka 588, Japan*
[25]*Universita di Padova, Istituto Nazionale di Fisica Nucleare, Sezione di Padova, I-35131 Padova, Italy*
[26]*University of Pennsylvania, Philadelphia, Pennsylvania 19104*
[27]*Istituto Nazionale di Fisica Nucleare, University and Scuola Normale Superiore of Pisa, I-56100 Pisa, Italy*
[28]*University of Pittsburgh, Pittsburgh, Pennsylvania 15260*
[29]*Purdue University, West Lafayette, Indiana 47907*
[30]*University of Rochester, Rochester, New York 14627*
[31]*Rockefeller University, New York, New York 10021*
[32]*Rutgers University, Piscataway, New Jersey 08855*
[33]*Academia Sinica, Taipei, Taiwan 11530, Republic of China*
[34]*Texas A&M University, College Station, Texas 77843*
[35]*Texas Tech University, Lubbock, Texas 79409*
[36]*Istituto Nazionale di Fisica Nucleare, University of Trieste/Udine, Italy*
[37]*University of Tsukuba, Tsukuba, Ibaraki 305, Japan*
[38]*Tufts University, Medford, Massachusetts 02155*
[39]*Waseda University, Tokyo 169, Japan*
[40]*University of Wisconsin, Madison, Wisconsin 53706*
[41]*Yale University, New Haven, Connecticut 06520*
(Received 22 February 1999; published 22 July 1999)

We present a measurement of the mass difference Δm_d of the two B_d^0 mass eigenstates. We use a flavor tagging method based on the lepton charge, in a sample of events with two muons at low transverse momentum. The sample corresponds to an integrated luminosity of 90 pb^{-1} collected by the Collider Detector at Fermilab. The result obtained is $\Delta m_d = 0.503 \pm 0.064(\mathrm{stat}) \pm 0.071(\mathrm{syst})$ ps^{-1}. [S0556-2821(99)50215-4]

PACS number(s): 12.15.Ff, 13.20.He, 14.40.Nd

The B_d^0 meson, a bound state of a $\bar{b}$ quark and d quark, is one of a few particles which can tranform from its particle state to the associated antiparticle state. This takes place via a second-order weak process involving an internal loop with two W bosons and two up-type (u,c,t) quarks coupling to the $\bar{b}$ and d quarks. By far the dominant contribution to this process comes from loops with top quarks, and so a measurement of the rate of $B_d^0 \leftrightarrow \bar{B}_d^0$ transitions is sensitive to the Cabibbo-Kobayashi-Maskawa (CKM) [1] matrix element

*Visitor.

V_{td} (while V_{tb} is assumed to be ≈ 1 due to unitarity constraints on the CKM matrix). Given a particle which is initially in a pure B_d^0 state, the probability of it decaying as a $\overline{B}_d^0$ at time t in its rest frame is

$$P(t) = \frac{e^{-t/\tau}}{2\tau}[1-\cos(\Delta m_d t)]$$

where τ is the average of the lifetimes of the two mass eigenstates of the B_d^0-$\overline{B}_d^0$ system [2]. Measuring the time evolution of this probability of a B_d^0 oscillating into a $\overline{B}_d^0$ requires a determination of the b-quark flavor (i.e., b or $\overline{b}$) of the B particle at both its production and decay times (flavor tagging), and the measurement of its proper decay time.

In this paper, we determine the mass difference Δm_d by measuring the frequency of oscillations of $B_d^0 \leftrightarrow \overline{B}_d^0$. The data used in this analysis were collected during the 1994–95 run of the Tevatron $p\overline{p}$ Collider, with the Collider Detector at Fermilab (CDF), and correspond to an integrated luminosity $\int \mathcal{L} dt \sim 90$ pb^{-1}. The sample consists of events containing two muons and at least one displaced vertex of tracks not consistent with coming from the primary interaction point. The distance between these vertices is used for the estimate of the decay length of the B candidate.

The charge of the muon in the semileptonic decay $b \rightarrow c\mu^-\overline{\nu}$ [3] is used to identify the flavor of the B at the time of its decay (where B refers generically to any particle, including baryons, containing a b or $\overline{b}$ quark). Since QCD processes produce B particles in pairs of opposite flavor, we infer the flavor at production of one B from the charge sign of the muon coming from the semileptonic decay of the other B.

The ability to perform precision b physics measurements at a $p\overline{p}$ collider has been demonstrated by CDF with the B lifetime measurements [4] and the determination of Δm_d [5]. These measurements have been obtained using fully or partially reconstructed B decay events, where the background calculations are rather straightforward, but the number of events is limited. In this paper, we show that a precise measurement of Δm_d is also possible using a more inclusive B meson identification. This provides a much larger data sample at the cost of a lower purity and a more complicated background evaluation.

The mass difference Δm_d is obtained by fitting for the oscillation frequency in a plot of the like-sign event fraction, $f_{\rm LS}(ct) = N_{\rm LS}(ct)/[N_{\rm LS}(ct) + N_{\rm OS}(ct)]$, where $N_{\rm OS}(ct)[N_{\rm LS}(ct)]$ is the number of events in which the two muons are of opposite (like) sign.

Since the b and $\overline{b}$ quarks hadronize and decay independently, each muon can come from several sources. First, the b quark can hadronize into a $\overline{B}_d^0$ which decays directly to a muon of negative charge, or into a $\overline{B}_d^0$ which oscillates to a B_d^0 and then decays directly to a muon of positive charge. Second, the b quark can hadronize into a B^- or Λ_b, and decay directly to a muon. Third, the b quark can hadronize into a $\overline{B}_s^0$, which can oscillate into a B_s^0, with a much higher frequency than a B_d^0 [6], effectively giving a random-sign muon. Fourth, for all of the above cases, the muon can also be produced in a sequential semileptonic decay $b \rightarrow c \rightarrow \mu^+\nu$, which has the exact opposite correlation of muon sign with b flavor from the above sources. Fifth, residual punch through or decay in flight of hadrons contribute to muon detection not related with a $b \rightarrow c\mu\nu$ decay. Finally, events with two muons can be generated by direct production and decay of charm. The shape of the $f_{\rm LS}$ histogram is then obtained by taking all possible combinations of two muons from these sources, weighted with the appropriate fractions of each source.

The CDF detector has been described in detail elsewhere [7]. Only the features most relevant to this analysis are reported here. CDF consists of a magnetic spectrometer surrounded by a calorimeter and muon chambers. The momenta of charged particles are measured up to a pseudorapidity [8] of $|\eta| < 1.1$ in the central tracking chamber (CTC), which is inside a 1.4 T superconducting solenoidal magnet. A low-noise, four-layer silicon microstrip vertex detector [9], located immediately outside the beampipe, provides precise track reconstruction in the plane transverse to the beam and is used to identify secondary vertices from b and c quark decays. The muon detection system (CMU) consists of drift chambers, located outside the calorimeter, allowing the reconstruction of track segments for penetrating particles. In this analysis, only the region up to $|\eta| < 0.6$ is used. An additional set of chambers (CMP), located outside a 0.6 m thick iron wall, provides additional information for the detection of muons. A three-level dimuon trigger selects events with two muons of transverse momentum $p_t > 2.2$ GeV/c, as measured by the Central Fast Tracker (CFT), a hardware track processor with a momentum resolution of $\delta p_t / p_t^2 = 0.03$ (GeV/c)$^{-1}$. At least one of the muons has to be detected in both the CMU and CMP drift chambers.

Offline muon identification is based on the three-dimensional matching of the track segment in the muon chambers with the segment reconstructed in the CTC and on the energy deposited in the calorimeter towers close to the muon trajectory. The invariant mass of the two muons is required to be greater than 5 GeV/c^2 in order to reject dimuons from the following sources: muons produced by the same B particle in a double semileptonic decay $b \rightarrow c\mu\nu, c \rightarrow s\mu\nu$; muons from a J/ψ decay; or muons from b's in gluon splitting to $b\overline{b}$. In addition, the transverse momentum relative to the beamline of each muon is required to be greater than 3 GeV/c. This requirement, almost fulfilled by muons detected both in the CMU and CMP, is motivated by the description of the fake muon contamination, as discussed later.

The algorithm used to find displaced vertices (presumed to be b or c quark decay vertices distinct from the primary one) is based on the correlation between the impact parameter d [10] and the azimuthal angle ϕ of tracks coming from these vertices. Tracks from a displaced vertex form a line in the d-ϕ plane with a non-zero slope, while tracks from the primary vertex will have a small d and show no obvious correlation with ϕ. A cluster is formed by three or more

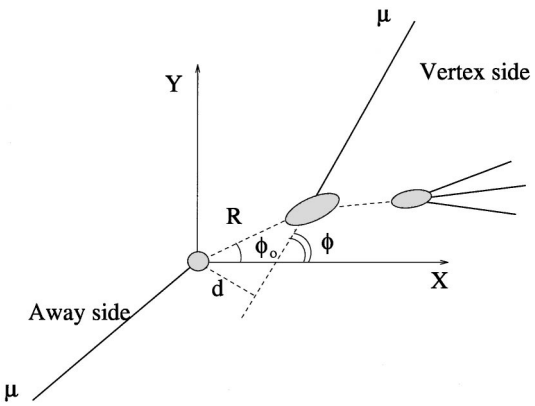

FIG. 1. Sketch of secondary vertex reconstruction scheme in a dimuon event. The primary vertex is represented in the figure as the origin of the *X*-*Y* axes. The impact parameter *d* and the azimuthal angle ϕ of tracks from a displaced vertex are related by $d = R \sin(\phi - \phi_0)$.

correlated tracks, with each (excluding muon tracks) having a significance $d/\sigma_d > 2$, where σ_d is the uncertainty on the impact parameter. At least one of the muons has to be associated with the cluster of tracks identified, regardless of its impact parameter significance. The tertiary vertex position (presumed to be the charm decay vertex) is then found by fitting all the tracks in the cluster excluding the muon track. The direction of the momentum obtained is extrapolated back from the vertex to the muon trajectory. The position of the intersection with the muon is taken as the seconday vertex (*B* candidate decay vertex). Figure 1 shows a sketch of the reconstruction method.

More than 95% of events in the selected sample have only one secondary vertex reconstructed: in the case of two secondary vertices reconstructed, only one is randomly picked up.

For each event, the proper decay length ct of one of the two *B*'s is determined by:

$$ct = L_{xy} \frac{m_{B_d}}{p_t} F(p_t, m_B^*)$$

where m_{B_d} is the *B* meson mass [6] and L_{xy} is the two dimensional decay length projected onto the direction of the transverse momentum of the cluster. The factor $F(p_t, m_B^*)$ is a correction based on a Monte Carlo simulation program of the $b\bar{b}$ production and decay process, passing the same selection as the real data. This factor is necessary due to the partial reconstruction of the *B* particle decay products. It is parametrized as a function of the reconstructed p_t and mass m_B^* of the *B* cluster defined by the set of tracks belonging to the d-ϕ cluster. The fraction of direct $b \to c\mu^- \bar{\nu}$ decays is enhanced with respect to charm decays to muons by requiring the momentum of the muon transverse to the momentum direction of the remaining tracks in the cluster (p_t^{rel}) to be greater than 1.3 GeV/c.

The sample selected amounts to 2044 like-sign dimuon events and 3924 opposite-sign events.

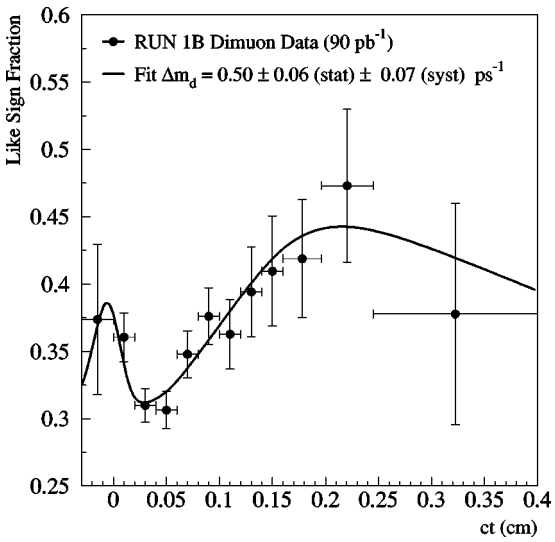

FIG. 2. Fraction $f_{\rm LS}$ of like-sign dimuon events as a function of proper decay length ct. Superimposed is the result of the χ^2 fit described in the text.

The fraction $f_{\rm LS}$ of events with like-sign muons is shown in Fig. 2 as a function of the proper decay length ct of the *B* particle with an identified secondary vertex. The rise for positive ct is due to the mixing, whereas the peak at the origin is an artifact of the larger fake contribution in this region.

The Monte Carlo simulation is based on the ISAJET generator [11] for the $b\bar{b}$ production process and fragmentation. The *B* particle decays are simulated with a different Monte Carlo program [12] based on measurements of branching fractions from CLEO experiment at the Cornell Electron-Positron Storage Ring (CESR) and experiments at the Large Electron Positron collider (LEP) at CERN [13]. A detailed simulation of the CDF detector and the reconstruction code is applied to each event. In addition, a simulation is used to replicate the trigger conditions for dimuon events. We used the HERWIG generator [14] as a check for possible effects on this analysis from a different fragmentation and hadronization modelling. The fraction $f_{\rm LS}$ is described with a model that takes into account the sample composition, resolution effects and the lifetime of *B* mesons. We use the simulation to parametrize the secondary vertex reconstruction efficiency, as a function of the reconstructed proper time, and the resolution in momentum and position of the vertex. The secondary vertex reconstruction efficiency is flat above one *B* lifetime. In addition, we correct the production fractions of *B* particle species, assumed equal to the ones measured at the CERN e^+e^- collider LEP [13], to account for the different analysis efficiencies of these species as determined in the simulation. Sequential $b \to c \to \mu^+$ decays constitute a major source of dilution of the mixing oscillation because they misidentify the *B* flavor. The fractions of sequential decays for muons on the secondary vertex side and for muons on the away side are determined using the Monte Carlo simulation, and the possible dependence of this fraction on the reconstructed proper time is also taken into account.

Two sources of background were investigated: fake iden-

TABLE I. Values of the parameters considered in the χ^2 fit.

Parameter	Input to fit	Output from fit
Δm_d		0.503 ± 0.077 ps^{-1}
τ_b	1.56 ± 0.06 ps	1.53 ± 0.04 ps
F_d	$(38.5 \pm 2.2)\%$	$(38.2 \pm 2.2)\%$
F_s	$(8.9 \pm 2.1)\%$	$(8.6 \pm 2.0)\%$
F_{bkg}	$(16.7 \pm 5.2)\%$	$(17.6 \pm 3.6)\%$

tification of muons and $c\overline{c}$ production. The fake muon contamination was studied on a sample of dimuon events in which one muon track is detected in the CMU chambers and extrapolates into the fiducial region of the CMP chambers, but is not detected there. This sample consists mainly of hadrons not interacting strongly in the calorimeter. The charge of the two particles detected as muons is completely uncorrelated and the absolute contributions to the sample of LS and OS events were verified to be the same within the errors. The ct distribution of these events was extracted taking into account the small contamination of real muons in the fake sample. In addition, from a comparison of the kinematic characteristics of this sample of misidentified muons and the Monte Carlo simulation of the $b\overline{b}$ signal, we determined the expected fraction of fake events in the data to be $F_{bkg} = (16.7 \pm 5.2)\%$. This study was based on the muon impact parameter, on the transverse component of the muon momentum with respect to the cluster of displaced tracks and on the invariant mass of the cluster. The last two variables were also defined with respect to a jet of tracks within a cone around the muon. The same study of the kinematic behavior of the data sample selected shows that the charm contribution is consistent with zero. The effect of possible residual charm contamination is considered in the discussion of the systematic effects in the measurement of Δm_d.

A χ^2 fit was then applied to the fraction $f_{\rm LS}$ of like-sign dimuon events, constraining the B particle lifetime to the value $\tau = 1.56 \pm 0.06$ ps [13], the fraction of B_d^0 mesons at $F_d = (38.5 \pm 2.2)\%$, the fraction of B_s^0 mesons at $F_s = (8.9 \pm 2.1)\%$ (these values are corrected for the species dependent efficiency), and finally, the fraction of events with fake muons at $F_{bkg} = (16.7 \pm 5.2)\%$ with a ct shape as determined above. The results obtained are reported in Table I, where the errors are the output from the fit. The χ^2 per degree of freedom of the fit is 1.1. The function used in the fit procedure to describe the fraction $f_{\rm LS}$ of like-sign dimuon events is superimposed on the data in Fig. 2.

The error on Δm_d returned by the fit is due to both the statistics and the errors assumed on the constrained parameters. We separate these two contributions in our final result, including the contribution from the uncertainty on τ_b, F_d, F_s and F_{bkg} in the systematic error. This separation has been done both analytically and by Monte Carlo with consistent results.

TABLE II. Systematic errors on Δm_d determination.

	$\delta(\Delta m_d)$(ps^{-1})
$\tau_b, F_d, F_s, F_{bkg}$	± 0.043
Fake shape	± 0.011
Sequential decays	± 0.048
$c\overline{c}$ contribution	$+0.027$
Resolution on L_{xy}	± 0.006
Resolution on p_t	± 0.001
Δm_s	$+0.003$
Parametrization of $F(p_t, m_B^*)$	± 0.009
Vertexing efficiency vs ct	± 0.006
Fitting procedure	-0.013

Table II summarizes the different sources of systematic errors on Δm_d, which have been estimated as follows. The uncertainties on the parameters constrained in the fit give a contribution of ± 0.043 ps^{-1}. The shape of the fake muon background has been parametrized independently of the $f_{\rm LS}$ like-sign fraction. Variations of this shape contribute less than ± 0.011 ps^{-1} to the Δm_d value. The fraction of sequential decays has been varied by $\pm 15\%$ with respect to the value obtained by the Monte Carlo and used in the fit, with a contribution of ± 0.048 ps^{-1}. The effect of a residual charm contamination was evaluated with a contribution of 2% and a variation of $\pm 20\%$ of the charm effective lifetime obtained from simulation. The resulting uncertainty is $+0.027$ ps^{-1}. From simulation, the bias of the fitting procedure on Δm_d has been evaluated to be -0.013 ps^{-1}. This bias is not used to correct Δm_d, but rather is considered as a contribution to the total systematic uncertainty. Finally, the other small effects listed in Table II are estimated by varying the corresponding contributions in the fit.

The total systematic uncertainty is obtained by adding all the contributions in quadrature. The final result is:

$$\Delta m_d = 0.503 \pm 0.064(\text{stat}) \pm 0.071(\text{syst}) \text{ ps}^{-1}.$$

This result is consistent with the world average [6] $\Delta m_d = 0.464 \pm 0.018$ ps^{-1}.

The overlapping of the sample used in this analysis with the one used in [5] is negligible.

We thank the Fermilab staff and the technical staffs of the participating institutions for their contributions. This work was supported by the U.S. Department of Energy and National Science Foundation, the Istituto Nazionale di Fisica Nucleare of Italy, the Ministry of Science, Culture, and Education of Japan, the Natural Sciences and Engineering Research Council of Canada, the National Science Council of the Republic of China, and the A.P. Sloan Foundation.

[1] N. Cabibbo, Phys. Rev. Lett. **10**, 531 (1963); M. Kobayashi and K. Maskawa, Prog. Theor. Phys. **49**, 652 (1973).

[2] In this formula, the relative difference between the widths of the two mass eigenstates has been neglected because, unlike the K^0-$\overline{K}^0$ system, it is expected to be very small in the B_d^0-$\overline{B}_d^0$ system [see A. J. Buras, W. Slominski, and H. Steger, Nucl. Phys. **B245**, 369 (1984)].

[3] Throughout this paper, charge conjugate modes are always implied.

[4] CDF Collaboration, F. Abe *et al.*, Phys. Rev. D **57**, 5382

(1998); CDF Collaboration, F. Abe *et al.*, *ibid.* **58**, 092002 (1998).

[5] CDF Collaboration, F. Abe *et al.*, Phys. Rev. Lett. **80**, 2057 (1998).

[6] Particle Data Group, C. Caso *et al.*, Eur. Phys. J. C **3**, 1 (1998).

[7] CDF Collaboration, F. Abe *et al.*, Nucl. Instrum. Methods Phys. Res. A **271**, 387 (1988).

[8] In the CDF coordinate system, θ and ϕ are respectively the polar and azimuthal angles with respect to the proton beam direction (z axis). Pseudorapidity η is defined as $\eta = -\ln[\tan(\theta/2)]$ with θ measured assuming a *z*-vertex position of zero unless otherwise noted.

[9] D. Amidei *et al.*, Nucl. Instrum. Methods Phys. Res. A **350**, 73 (1994); P. Azzi *et al.*, *ibid.* **360**, 137 (1995).

[10] The impact parameter *d* is the distance of closest approach of a track with respect to the primary vertex in a plane tranverse to the beam direction. In this analysis, the particles detected as muons were not included in the reconstruction of the primary vertex.

[11] F. Paige and S. D. Protopopescu, BNL Report No. 38034, 1986.

[12] P. Avery, K. Read, and G. Trahern, Cornell Internal Note CSN-212, 1985.

[13] Particle Data Group, R. M. Barnett *et al.*, Phys. Rev. D **54**, 1 (1996).

[14] G. Marchesini *et al.*, Comput. Phys. Commun. **67**, 465 (1992).